NSWC TR 79-119

LEVEL
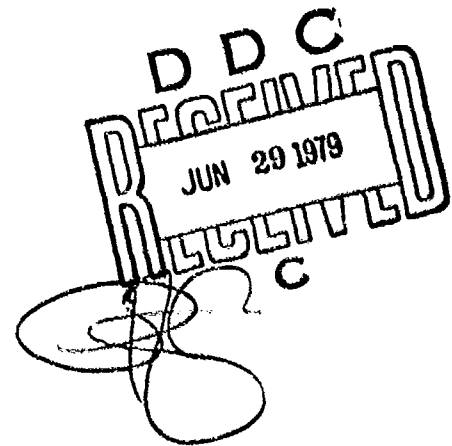
DEFLAGRATION TO DETONATION TRANSITION BEHAVIOR OF ALUMINIZED HMX

BY   DONNA PRICE   A. R. CLAIRMONT, JR

RESEARCH AND TECHNOLOGY DEPARTMENT

4 JUNE 1979

NAVAL SURFACE WEAPONS CENTER

Dahlgren, Virginia 22448 ● Silver Spring, Maryland 20910

REPORT DOCUMENTATION PAGE	READ INSTRUCTIONS BEFORE COMPLETING FORM

1. REPORT NUMBER NSWC-TR-79-119	2. GOVT ACCESSION NO.	3. RECIPIENT'S CATALOG NUMBER

4. TITLE (and Subtitle) DEFLAGRATION TO DETONATION TRANSITION BEHAVIOR OF ALUMINIZED HMX	5. TYPE OF REPORT & PERIOD COVERED
	6. PERFORMING ORG. REPORT NUMBER

7. AUTHOR(s) Donna Price A. R. Clairmont, Jr.	8. CONTRACT OR GRANT NUMBER(s)

9. PERFORMING ORGANIZATION NAME AND ADDRESS Naval Surface Weapons Center White Oak Silver Spring, Maryland 20910	10. PROGRAM ELEMENT, PROJECT, TASK AREA & WORK UNIT NUMBERS 61152N, ZR00001 ZR01305, R0116

11. CONTROLLING OFFICE NAME AND ADDRESS	12. REPORT DATE 4 June 1979
	13. NUMBER OF PAGES 42

14. MONITORING AGENCY NAME & ADDRESS(If different from Controlling Office)	15. SECURITY CLASS. (of this report) UNCLASSIFIED
	15a. DECLASSIFICATION/DOWNGRADING SCHEDULE

16. DISTRIBUTION STATEMENT (of this Report)

Approved for public release, distribution unlimited.

17. DISTRIBUTION STATEMENT (of the abstract entered in Block 20, if different from Report)

18. SUPPLEMENTARY NOTES

19. KEY WORDS (Continue on reverse side if necessary and identify by block number)

DDT	Aluminized HMX
Detonation	Combustion
Sensitivity	Flame Spreading
Explosives	

20. ABSTRACT (Continue on reverse side if necessary and identify by block number)

The effect of fine (5μ) and coarse (95μ) Al on the deflagration-to-detonation (DDT) behavior of HMX, in charges pressed to 90% theoretical maximum density (TMD), was studied. It was found that Al slows down the DDT process increasingly as the content of Al increases; that is, it increases predetonation column length and the relative times to detonation. Fine Al is more effective than coarse in delaying DDT, at a given content, but both are inferior to wax in this respect.

DD FORM 1473 EDITION OF 1 NOV 68 IS OBSOLETE
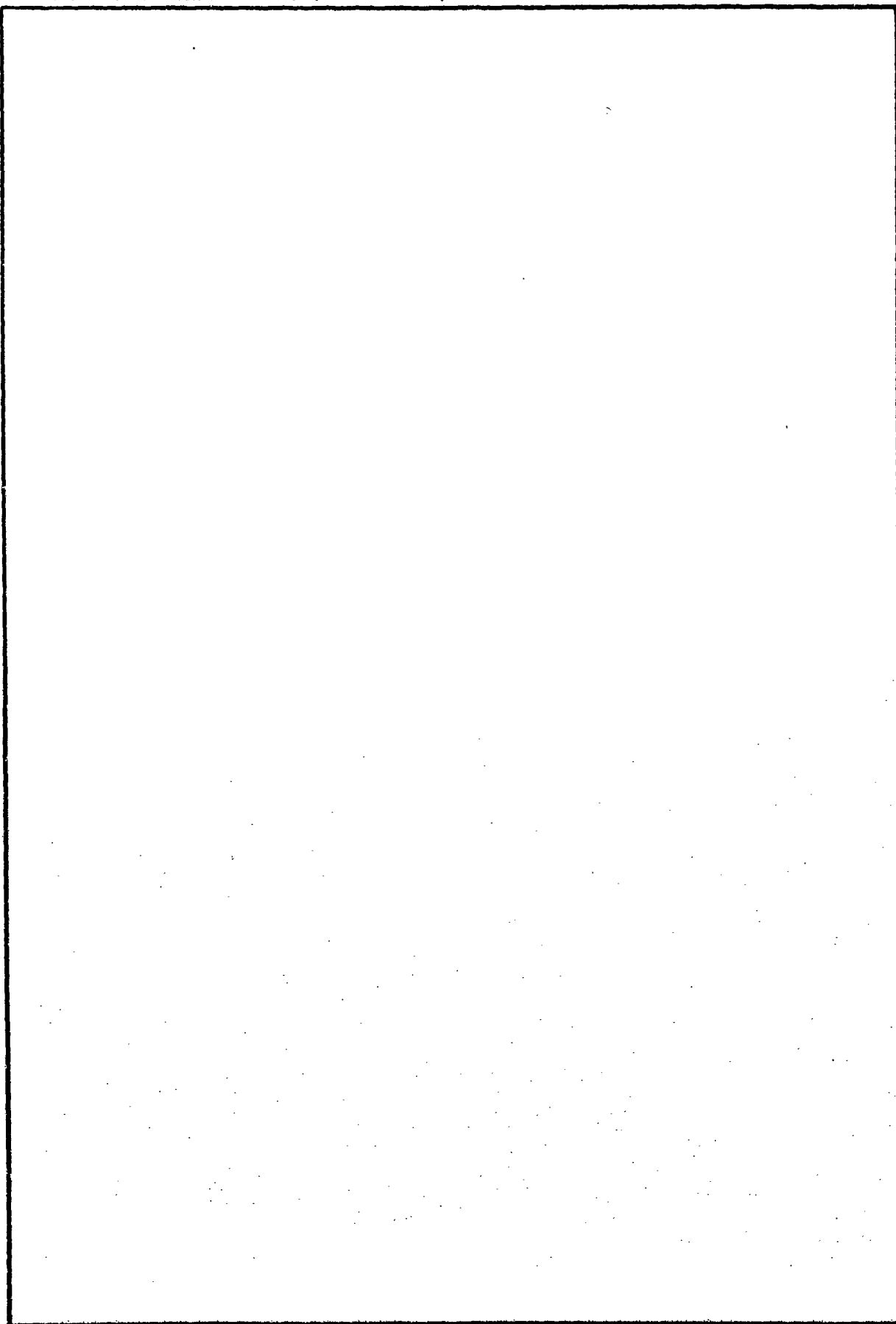1 JAN 73

S/N 0102-LF-014-6601

SUMMARY

The effect of fine (5μ) and coarse (95μ) Al on the deflagration-to-detonation (DDT) behavior of HMX, in charges pressed to 90% theoretical maximum density (TMD), was studied. It was found that Al slows down the DDT process increasingly as the content of Al increases; that is, it increases predetonation column length and the relative times to detonation. Fine Al is more effective than coarse in delaying DDT, at a given content, but both are inferior to wax in this respect.

JULIUS W. ENIG
By direction

CONTENTS

ILLUSTRATIONS

ILLUSTRATIONS (Cont.)

TABLES

INTRODUCTION

Although studies of deflagration-to-detonation transition
(DDT) have been underway for some years, the transitional behavior
in aluminized explosives has been very little studied. Moreover,
relatively few pressed explosives have been examined for DDT
at porosities as low as 10%. Those reported are PETN,[1] possibly
HMX,[2] and several pure and waxed HE studied in our Laboratory.
It is the purpose of this report to present the results of a
study of aluminized HMX at 90% theoretical maximum density (TMD).
Hence this work supplies much needed data on both aluminized
and highly compacted HE.

The composition range was 10-40% Al. Series were prepared
with two different particle sizes of Al (5 and 95μ) to study the
effect of that parameter on the transitional behavior. All mixtures
which exhibited transition followed the DDT mechanism of Reference 3
with the exception of the convective flame front. This front
was not detected in most mixtures at 90% TMD; however, the mixtures
of 75/25 and 70/30 HMX/5μ-Al did show initial front velocities
as low as 1.1 mm/μs.

EXPERIMENTAL ARRANGEMENT AND PROCEDURE

The experimental setup and procedures have been described
in detail elsewhere.[3,4] The apparatus consists of a seamless steel

---

[1]Korotkov, A. I., Sulimov, A. A., Obmenin, A. V.,
Dubovitskii, V. F., and Kurkin, A. I., "Transition from Combustion
to Detonation in Porous Explosives," Combustion, Explosion, and
Shock Waves 5, 317 (1969).

[2]Griffiths, N. and Groocock, J. M., "The Burning to Detonation
of Solid Explosives," J. Chem. Soc., 4154, 1960.

[3]Bernecker, R. R. and Price, D., "Studies in the Transition
from Deflagration to Detonation in Granular Explosives," Combust.
Flame 22, 111-117, 119-129, and 161-170 (1974). See also Naval
Ordnance Laboratory TR 72-202.

[4]Price, D. and Bernecker, R. R., "Sensitivity of Porous
Explosives to Transition from Deflagration to Detonation," Combust.
Flame 25, 91-100 (1975). See also Naval Ordnance Laboratory
TR 74-186.

tube with heavy end closures. The column length of the 0.35 g of 25/75 B/KNO$_3$ ignitor is 6.3 mm; the length of the explosive column is 295.4 mm. Each charge is examined by x-ray prior to its instrumentation.

The DDT tube is instrumented with ionization probes (IP) and strain gages (SG) to monitor ionization fronts and internal pressure, respectively. For brevity, henceforth ionization probes will be referred to as probes; strain gages, as gages. As before,[3] both custom-made and commercial probes are used; distance-time (x-t) data from each are distinguished on the graphs. The number of gage locations for monitoring internal pressure is generally four or five per tube. The gage output is reported in strain (ϵ) or microstrain ($\mu\epsilon$). In a static calibration of the tube, the gradient is 112 $\mu\epsilon$/kbar up to the elastic limit at 2.2 kbar. From 2 to 4.7 kbar, the microstrain increases from 225 to 788.

One difference in procedure from that reported in Reference 3 is in the determination of the predetonation column length, ℓ. In the case of 91/9 RDX/wax, it was possible to use the intersection of the postconvective wave front with the extrapolated detonation front to locate ℓ in the x-t plane; the value was confirmed by that obtained from tube fragments. Here, and in general for HE other than 91/9 RDX/wax, ℓ is more reliably determined from markings on the tube fragments; it is checked for consistency with the probe and gage records in the x-t plane. Unless otherwise indicated, ℓ values are measured to $\pm$ 3 mm.

The HMX used was Class A ($\bar{\delta}$~200μ); it satisfied the relevant military specification and had the identification number X906. Spherical aluminum powder was obtained from the Valley Metallurgical Processing Company and the Naval Ordnance Station, Indian Head, Maryland. The two batches, designated H5 and H95, had the respective nominal particle sizes of 5 and 95μ. The mixing procedure was that used in Reference 4 for one kg batches.

EXPERIMENTAL RESULTS AND DISCUSSION

Eleven shots were made: one on 70% TMD HMX, five on the coarse Al mixtures, and five on the fine Al mixtures. Detailed tables, records for each shot, and discussions of them appear in the Appendix. Table 1 contains a summary of these data.

SG records of these shots were examined carefully for any features which consistently differed from those of records from more porous charges. Because of the lower porosity we thought it possible that these charges might transmit more stress to the tube walls through the solid explosive rather than from gas pressure on the walls. However, no distinctive difference was found in these SG records as compared to those obtained on charges of %TMD $\leq$ 70.

Table 1. Summary of Data on Effect of Aluminum on DDT of HMX[a]

Shot No.	%Al	ρ_0 g/cm³	%TMD	Al/O	ℓ mm	$29\Delta t_D$ μs	$29\Delta t_E$ μs	D mm/μs
105?	0	1.32	69.6	0.0	41	2	12	7.0
H95 Al								
102C	10	1.76	89.7	0.153	105.0	25.6	42.6	8.3
113C	10	1.77	90.4	0.153	47.8	8.5	9.5	8.3
101C	20	1.82	90.2	0.343	56.6	9.4	9.4	8.3
103C	30	1.86	89.1	0.588	78.2	25.3	26.1[e]	8.0
108C	40	1.94	90.0	0.915	59.2	17.8	17.8	7.7
H5 Al								
111C	10	1.78	90.9	0.153	56.4	10.8	16	8.0
107C	20	1.83	90.5	0.343	92.2	31.0	35.8	8.0
112C	25	1.85	90.4	0.458	149.4	74.0[d]	60.5	8.2
110C	30	1.89	90.4	0.588	295[d]	120.0[d]	106.5[d]	b
106C	40	1.96	90.8	0.915	-	-	-	F(c)

a. $29\Delta t_D$ is the relative time to detonation referred to the time of discharge of an IP at x = 29 mm. Similarly, $29\Delta t_E$ is the relative time from the arrival of a compression wave at x = 29 mm to the onset of detonation.

b. Charge failed to show steady state detonation, but was rapidly approaching it. See Figure A10a. In view of the velocity data, the lack of a clear demarkation on the tube wall, it has been assumed that onset occurred at the very end of tube.

c. All instrumentation failed on this shot, but it was clear from the tube fragmentation that transition had not occurred. See Figure A11.

d. Estimate and lower limit of actual value.

e. Correction from Δt_D to Δt_E appeared negligible because of the location of first compression front.

In 90% TMD 91/9 RDX/wax, the first compressive front, as outlined by SG data, occurred behind the first ionized front (IP detection) which travelled at about 0.6 mm/µs.[3] In 90% TMD 94/6 RDX/wax, the first compressive front occurred ahead of the IP front which travelled at about 1 mm/µs.[5] The 90% TMD aluminized HMX mixtures gave space-time diagrams resembling those of the corresponding 94/6 RDX/wax mixture. The first front detected by the IPs had velocities ranging from 1.1 (at high Al contents) to about 3 mm/µs. These values are too high for convective fronts; they are probably associated with pressure induced reactions.

Figure 1 shows the space-time diagram for 75/25 HMX/5µ-Al. It is probably the best record of the series because the high aluminum content has spread out the process so that more features can be resolved. We believe it shows the typical DDT behavior in all the aluminized mixtures although the features are not as well resolved in other records. Note that the rate of discharge of the IPs is accelerating from a velocity of 1.1 mm/µs. The first detected compression front starts slightly later and in the region near the ignitor; it travels at 2.2 mm/µs (a reasonable sound speed for this material), rapidly overtakes and passes the IP front which then speeds up to travel at about 2.1 mm/µs. The reaction responsible for the initial acceleration of the IP front has evidently occurred before the first IP responds. Although a convective flame front was not detected, the transition seems to follow the DDT model originally proposed,[3] i.e., accelerated burning leading to a series of compressive waves which coalesce to form a shock of sufficient strength to initiate detonation.

Figures 2-4 show the effect of aluminum particle size and content on the DDT parameters, predetonation column length (ℓ), relative time to detonation (Δt_D), and the interval between the formation of the first compressive front and the onset of detonation (Δt_E).* The relative times (See Table 1) have been taken for a probe positioned at $x = 29$ mm; the first probe was located at 22 or 29 mm for these shots rather than at the more customary 41 mm. These figures show quite clearly that all three DDT parameters increase with increasing %Al and that the fine Al is much more effective in causing the increase than is the coarse.

_____

[5]Price, D. and Bernecker, R. R., "DDT Behavior of Waxed Mixtures of RDX, HMX, and Tetryl," NSWC/WOL TR 77-96, 18 Oct 1977.

*Note that Δt_D is determined entirely by IP measurements whereas Δt_E is determined chiefly by SG data.
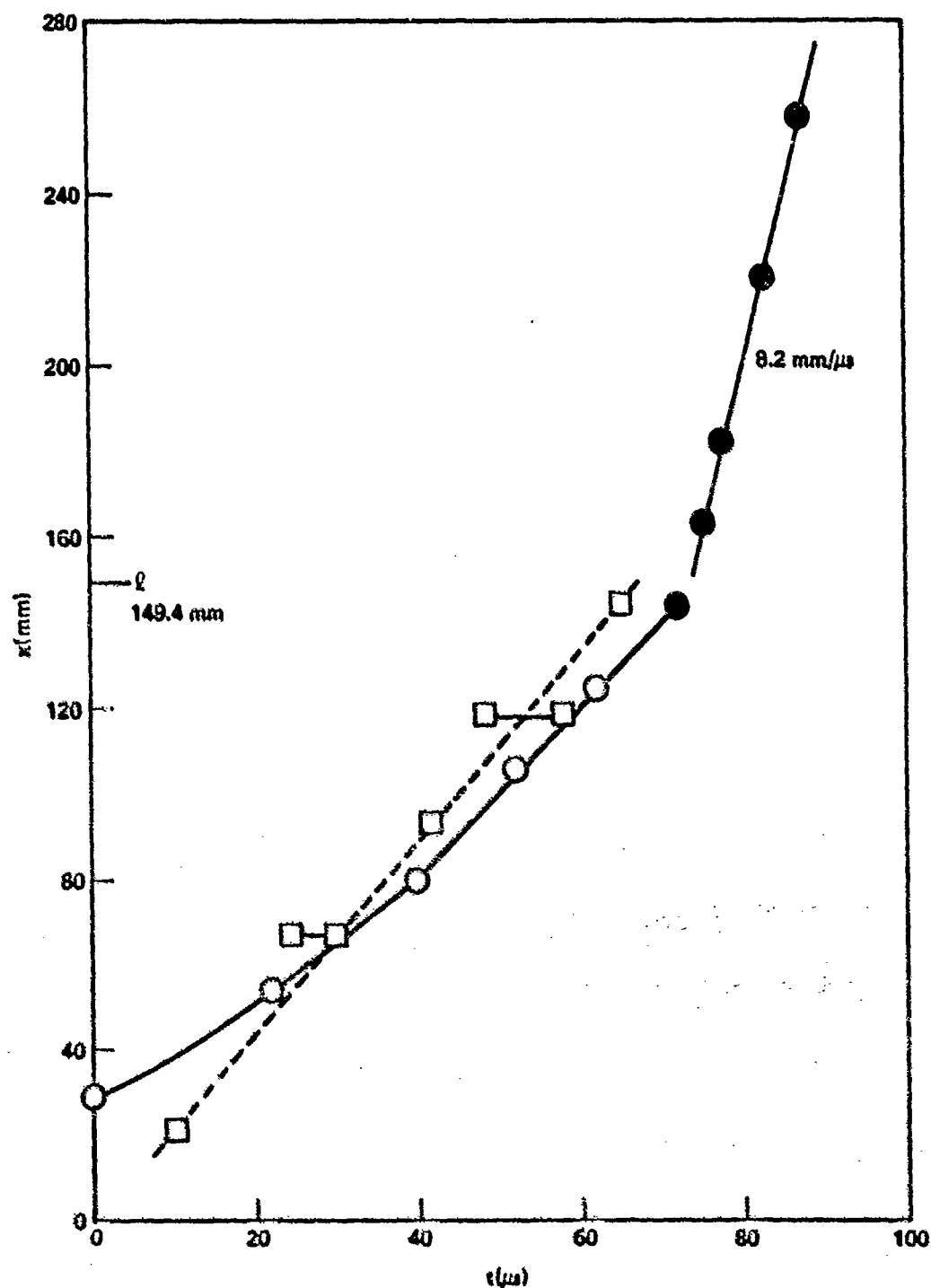
FIGURE 1   SHOT 112C ON 90.3% TMD 75/25 HMX/Al, $\rho_o = 1.85$ g/cm^3 DISTANCE-TIME DATA.
(◯ WOL PROBES, ● COMMERCIAL PROBES, ☐ SG EXCURSION TIME)
SEE ALSO FIGURE A9.

8

The estimated value for the mixture containing 30% fine Al is a lower limit. In other words, the experimental result was $\ell \geq 295$ mm. Hence all data points marked with an asterisk are estimates that might well be lower than the actual value. The Appendix discusses this and the scatter of the data for the mixtures containing coarse Al. In the latter case, two obvious factors might contribute: (1) the mixing procedure seemed less effective with the coarse Al than the fine, i.e., the final mixtures appeared less uniform; and (2) the compaction process during charge preparation had produced a number of demonstrably poor charges. X-ray examination through a thick-walled, steel tube is, however, an insensitive measure of charge uniformity, and might easily fail to detect flaws which could influence DDT. Thus data from one of the charges containing 10% 95μ Al (No. 102C) were omitted when fitting the curves of Figures 2-4 because they contradict the trend for the effect of increasing Al shown by both coarse and fine Al. We believe that the result for 40% Al is low and that for 30% Al about right. However, since the curves can be, and have been, drawn between these two points without changing the qualitative trend, repeat shots did not seem justified.

In a recent report[5] it was shown that waxed Class A RDX and waxed Class A HMX fall on the same curve, ℓ vs %wax, when both charges are at 70% TMD. Assuming that equivalent behavior is also evident at 90% TMD, we can use the data for 91/9 RDX/wax and 94/6 RDX/wax at 90% TMD[5] to compare the effects of Al and wax on HMX. In this way we find that 20-21% 5μ-Al and > 30% 95μ-Al in HMX have about the same values of ℓ, Δt_D, and Δt_E as 6% wax in HMX. Similarly, 25% (or more) 5μ-Al results in ℓ and Δt values close to those for 9% wax. In other words, on a weight basis, wax is far more effective in slowing down the transition than is Al. It is also more effective on a volume basis although the difference is not great.

In Figures 2-4, curves for both fine and coarse Al extrapolate to about the same value for 0% Al, or for 90% TMD HMX, as they should. A 90% TMD charge of HMX was not run because we did not want it prepared on the hydraulic press at this time. The extrapolated values were not very different from the experimental value of 70% TMD HMX which was run to check the new batch of HMX. The latter value is shown on the figures.

Both from the shape of the curves and parallel knowledge of waxed RDX, a good correlation between Δt_E and ℓ would be expected. This is indeed the case as Figure 5 shows; moreover the scatter of Figures 2-4 has been eliminated. If the one estimated point is too low, the curve may be linear as was the case for a smaller range in the waxed RDX.[5]

FIGURE 3 RELATIVE TIME TO DETONATION
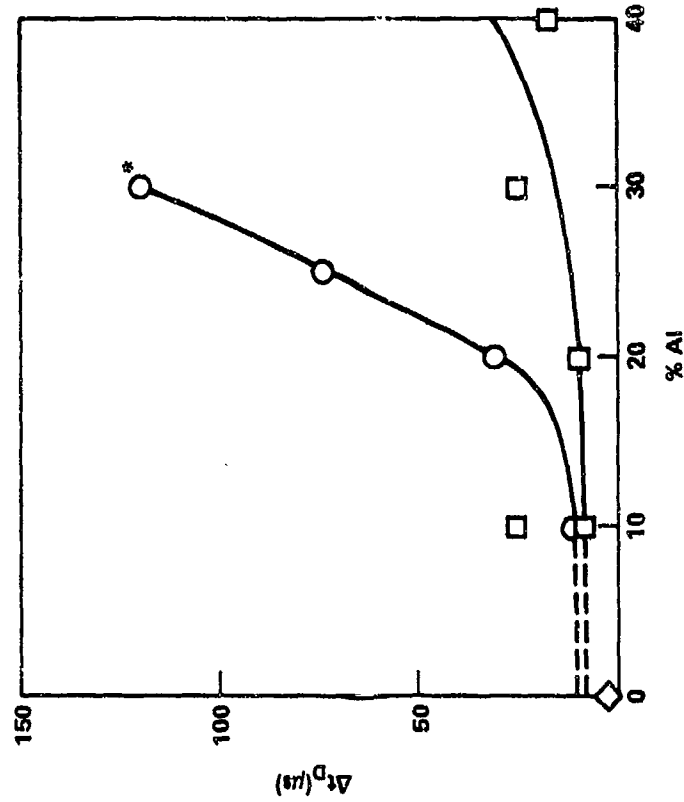VS ALUMINUM CONTENT FOR 90%
TMD HMX/Al.(○ 5μAl; □ 95μAl;
◇ 70% TMD HMX; *ESTIMATED VALUE.)
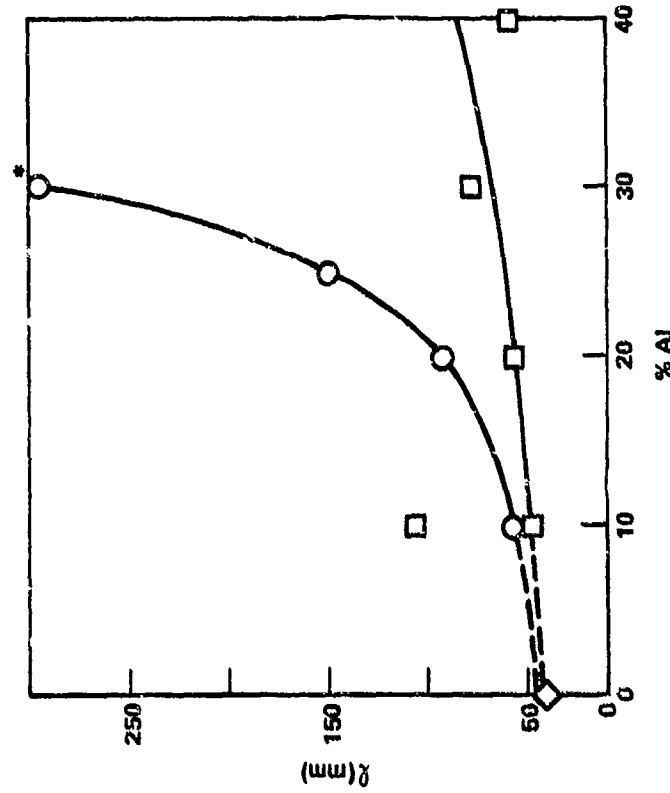
FIGURE 2 PREDETONATION COLUMN LENGTH
VS ALUMINUM CONTENT FOR 90%
TMD HMX/Al., ○ 5μAl; □ 95μAl;
◇ 70% TMD HMX; *ESTIMATED VALUE.)

10

FIGURE 5   RELATIVE TIME Δt_E VS PREDETONATION COLUMN LENGTH FOR 90% TMD HMX/Al. (O 5μAl; □ 95μAl; ◇ 70% TMD HMX; *ESTIMATED VALUE.)

FIGURE 4   RELATIVE TIME Δt_E VS ALUMINUM CONTENT FOR 90% TMD HMX/Al. (O 5μAl; □ 95μAl; ◇ 70% TMD HMX; *ESTIMATED VALUE.)

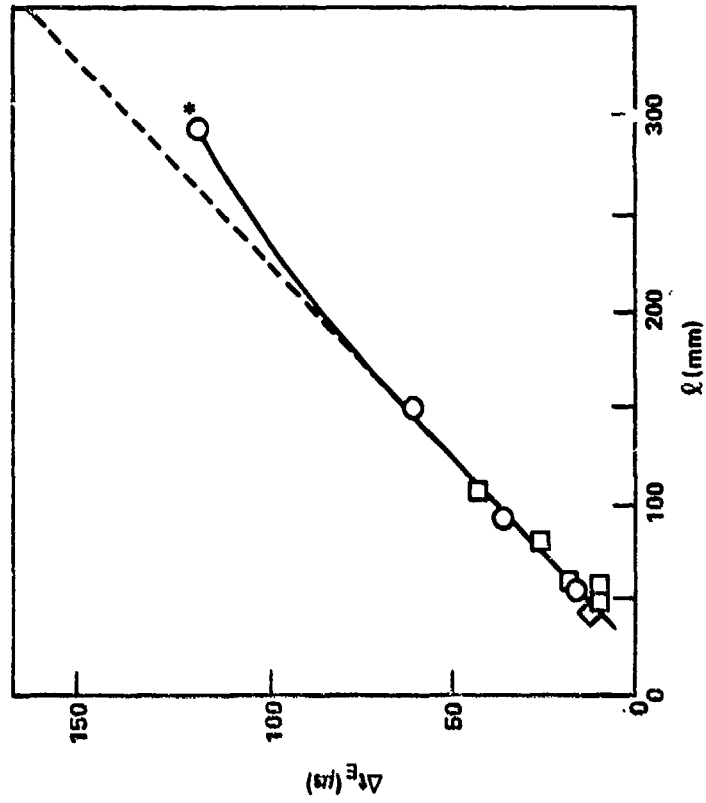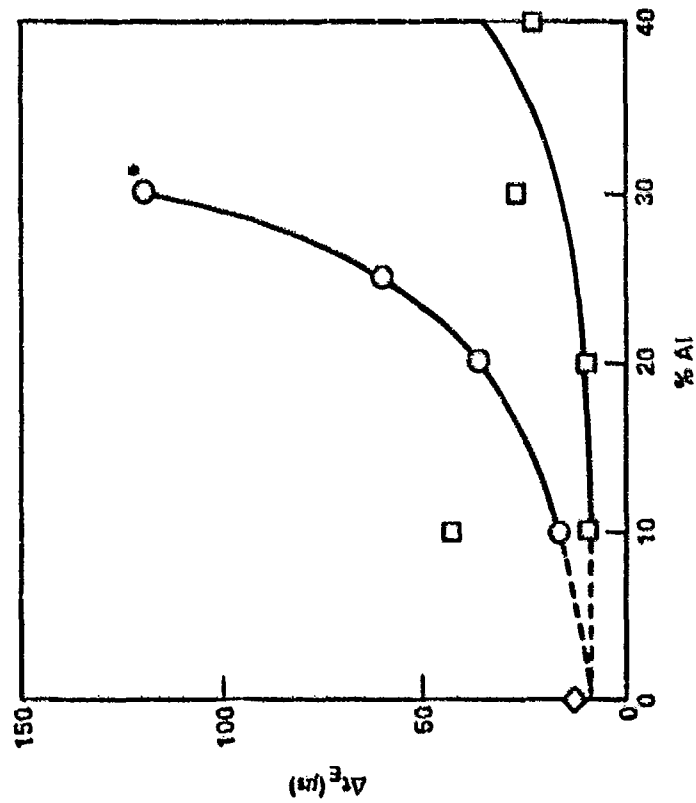The curve of Figure 5 suggests that Δt_E is a function of ℓ and independent of both Al particle size δ and aluminum concentration. For the waxed RDX and the waxed HMX series at 70% TMD, over the range of $\ell \leq 140$ mm, Class A RDX. Class A HMX, and 115μ-HMX all fell on the same curve, Δt_E vs ℓ, within experimental error.[5] However, data at $\ell > 140$ mm indicated separate curves for the two HMXs and possibly for the RDX as well; the difference was small and became smaller as ℓ decreased.* Hence the HMX particle size effect on the relation is negligible at $\ell \leq 140$ and small (if significant) at $\ell > 140$. It is not inconsistent with a negligible effect of Al particle size, in aluminized series, as shown in Figure 5.

In all of the waxed HE,[5] data points appeared on the Δt_E vs ℓ curve in order of increasing ℓ which corresponded to the order of increasing diluent. This is also true of the fine Al series shown in Figure 5. For the coarse Al series, there was much scatter (Figures 2-4). Hence these points (squares in Figure 5) do not appear in the order of increasing %Al, but are in a random order. Their location near the curve might be fortuitous.

At 90% TMD, aluminum would not be expected to have much effect on the detonation velocity.[6,7] For about 30% Al in RDX, the decrease in D should be about 5% or 0.4 mm/μs. Table 1 shows a decrease of 0.3 mm/μs for this concentration of coarse Al and none (or an increase) for the fine. The size of the effect is just about that to be expected from experimental error so that it cannot be considered of much significance.

Finally, it is of interest that the mixtures with coarse aluminum caused greater fragmentation damage (smaller fragments and more of them) than did mixtures with fine aluminum. The former behaved more like the pure explosive than the latter in both DDT and fragmentation.

---

[6]Price, D., "Aluminized Organic Explosives," NOLTR 72-62, 8 June 1972.

[7]Price, D., Clairmont, Jr., A. R., and Erkman, J. O., "Explosive Behavior of Aluminized AP," NOLTR 72-15, App. B & C, 2 May 1972.

*On the other hand, waxed RDX had distinctly different Δt_E vs ℓ curves at 70% and 85% TMD;[5] this difference is large and it is also one reason that series of constant composition HE with varying degrees of compaction fail to show a correlation between Δt_E and ℓ.

SUMMARY AND CONCLUSIONS

1. Addition of fine (5μ) and coarse (95μ) aluminum to HMX, in charges at 90% TMD, increases predetonation column length (ℓ) and the relative times to detonation (Δt_D, Δt_E).

2. All three DDT parameters increase with increasing %Al. They are interdependent and a good correlation exists between Δt_E and ℓ.

3. Al causes only a small decrease in detonation velocity D at 90% TMD.

4. Strain gage records from the 90% TMD charges showed no features different from those previously obtained on charges of higher porosity.

REFERENCES

1. Korotkov, A. I., Sulimov, A. A., Obmenin, A. V., Dubovitskii, V. F., and Kurkin, A. I., "Transition from Combustion to Detonation in Porous Explosives," Combustion, Explosion, and Shock Waves 5, 317 (1969).

2. Griffiths, N. and Groocock, J. M., "The Burning to Detonation of Solid Explosives," J. Chem. Soc., 4154, 1960.

3. Bernecker, R. R. and Price, D., "Studies in the Transition from Deflagration to Detonation in Granular Explosives," Combust. Flame 22, 111-117, 119-129, and 161-170 (1974). See also Naval Ordnance Laboratory TR 72-202.

4. Price, D. and Bernecker, R. R., "Sensitivity of Porous Explosives to Transition from Deflagration to Detonation," Combust. Flame 25, 91-100 (1975). See also Naval Ordnance Laboratory TR 74-186.

5. Price, D. and Bernecker, R. R., "DDT Behavior of Waxed Mixtures of RDX, HMX, and Tetryl," NSWC/WOL TR 77-96, 18 Oct 1977.

6. Price, D., "Aluminized Organic Explosives," NOLTR 72-62, 8 June 1972.

7. Price, D., Clairmont, Jr., A. R., and Erkman, J. O., "Explosive Behavior of Aluminized AP," NOLTR 72-15, App. B & C, 2 May 1972.

APPENDIX A

DETAILED DATA FOR ALL SHOTS

Measurements for all shots are given in Table Al. The
distance-time plot and the strain-time plot, where available,
are displayed in Figs. Al-Al0 as parts a and b, respectively.
Fig. All shows the effect of Al concentration on tube fragmenta-
tion, and supplements Figs. A7-Al0 for 5μ Al.

<u>HMX</u>

Fig. Al displays the data for the current batch of HMX of
70% TMD. Its short accelerating convective flame front (0.5 mm/μs)
followed and then preceded by a compressive front (at 1.6 mm/μs)
compares very well, i.e., almost reproduces, the data for 70% TMD
RDX and HMX given in reference 5. There RDX had an initial front
velocity of 0.5 mm/μs followed by PC front at 1.3-1.5 mm/μs (see
Ref. 5, Fig. 4). Similarly HMX (Ref. 5, Fig. Dll) exhibited
analogous velocities of 0.4 mm/μs and 1.3 mm/μs. In each case,
the compressive wave originated behind the convective front and
near the ignitor/explosive interface. It then overtook and passed
the convective front. The apparent DDT mechanism was in each case
that proposed in Reference 3. Evidently Batch X906 shows behavior
equivalent to that of previous batches of Class A RDX and HMX.

<u>Mixtures with 95μ-Al</u>

Mixtures with the coarser aluminum were harder to prepare,
i.e., they seemed less uniform, than those made with the finer
aluminum. Their records were also somewhat more difficult to
read and interpet.

Fig. A2 shows data from the first shot on 90/10 HMX/Al.
Although much of the SG records was obscured by interaction between
the IP discharges and the SG, two compression fronts were observed:
one preceding the front detected by IPs (the common order found in
this study) and one almost coincident with it. See Fig. A2a. The
velocities of all three fronts were much the same, and, at 3 mm/μs,
higher than the estimated sound velocity of the original charge.

Fig. A3 displays data from the shot of a second 90/10 HMX/Al
charge. The SG records are cleaner, but because of the very short
predetonation column length, only two pressure excursions were
detected: one ahead of the front outlined by IPs (the usual
location) and one obviously responding to the detonation. See Fig.
3Aa. Again the initial IP front has a velocity (2.7 mm/μs) to be
expected of a compressive wave, and the discharge of the IPs is
attributed to a pressure induced reaction.

Although these charges show satisfactory replication in the
detonation region, they are thoroughly unsatisfactory in repro-
ducing the predetonation column length ℓ. The cause of the different
predetonation behavior is attributed to differences in charge
preparation not detectable by x-ray examination and possibly to

differences in uniformity of the mixture as well. Predetonation
phenomena of non-steady combustion would be far more sensitive to
small physical differences in the charge than would detonation.

Data from the 80/20 HMX/Al charge are shown in Fig. A4. This
is the first case in which the pressure excursion is shown as
squares connected by a line. Here the squares indicate the boundary
of a region within which the excursion occurred. As Fig. A4b shows,
limits rather than a single point are required here because (1)
interaction of IPs with SG obscures portions of the record and (2)
irregularities appear in the record of SGs located at or near the
point of detonation onset. The last two excursions are the result
of the detonation; in fact, the next to the last SG (x=56.8 mm) is
at the point of onset of detonation (ℓ=56.6 mm). The first two
excursions show a pattern of the compression wave originating
behind the front outlined by IP response; this front is accelerating
and travelling at a higher velocity so that it overtakes the IP
front. A similar pattern was observed in the higher % TMD waxed
explosives (5), and is probably not detected in most of the aluminized
HE because the triggering IP responds too late. The presense of Al
probably lowers the temperature and hence the concentration of charged
particles below the level necessary for probe response.

The Fig. A5 for 70/30 HMX/Al, the compression wave ($\sim$3 mm/μs)
has been drawn in a pattern similar to that of Fig. A4. However,
two parallel compression fronts sandwiching the IP front could have
been drawn through the data from the first three SGs. The record
for the last, which happened to be at the point of detonation onset,
clearly shows the dip in the strain-time record associated with the
passage of a strong shock (See Fig. A5b). The corresponding
pressure excursion therefore belongs where it falls in Fig. A5a at
the beginning of the detonation region.

In Shot 108C on 60/40 HMX/Al, the SG records were lost. Hence
Fig. A6 consists of only the distance-time diagram with no compression
fronts shown. The initial velocity, obtained from the IPs is 1.4
mm/μs, the lowest observed in this series.

Mixtures with 5μAl

From Fig. A7 on, the data displayed are those obtained from
mixtures of HMX with fine aluminum. Very few new features appear
in these shots, but their results do permit some generalizations.
For example, all the IP fronts are of somewhat lower velocity than
those of the comparable mixture with coarse Al.

Fig. A7 for 90/10 HMX/Al needs no special comment except that
the response of the SG at x$\sim\ell$ is exactly what might be expected for
the passage of a shock (in this case, a detonation): a rapid rise
in strain followed by a fairly rapid decay and gage destruction.
As was pointed out in several earlier records, more often we observe
a sharp dip rather than a sharp rise in the presence of a shock.

A-2

Thus Fig. A8b at the SG just ahead of $x=\ell$ shows a sharp dip in the data from 80/20 HMX/Al. However the SG just beyond $x=\ell$ shows two dips followed by a very large and rapid rise.

Fig. A9a for 75/25 HMX/Al shows a better example of the same pattern noted in Fig. A4a, that which every charge might show with earlier IP response. Here $\ell=149$ mm and the SG at 118 mm shows a very sharp rise, followed by decay; that at 143 mm shows only minor disturbances until its final rapid rise.

Fig. A10 for 70/30 HMX/Al shows that this charge may not have detonated before the end of the tube. However, the displacement of the IP datum at 117 mm and the monotonic increase in front velocity thereafter indicate that the detonation velocity ($\sim$8 mm/μs) might have been achieved just at the end of the tube. That plus the fact that the closure bolt was heavily dented seem to justify an estimate of $\ell \sim 295$ mm. This cannot, of course, be justified by tube markings.

All records were lost for the shot on 60/40 HMX/Al, but from data on the previous shot, lack of tube marking, and type of fragments, this shot certainly did not reach detonation although there was a dent in the closure bolt. Fig. A11 shows fragments from Shots on 90/10 and 75/25 HMX/Al (which detonated) as well as for 70/30 which may just have reached detonation and for 60/40 HMX/Al which failed. It is quite evident that fragmentation efficiency decreased as aluminum content increased whether or not a detonation occurred.

TABLE A1
DETAILED DATA FOR SHOTS

Shot No.	109C		102C		113C	
HE	HMX[a]		90/10 HMX/Al[c]		90/10 HMX/Al[c]	
$\rho_0(\rho_v)$, g/cm^3	1.322(1.900)		1.756(1.958)		1.771(1.958)	
% TMD	69.6		89.7		90.4	
IP Data	x	t	x	t	x	t
	3.30	0.0*	22.35	0.0*	22.35	0.0*
	16.00	23.4*	35.05	5.4*	35.05	4.6*
	28.70	28.9*	47.75	8.5*	47.75	9.5*
	41.40	30.8*	60.45	12.8*	60.45	11.3*
	54.10	32.5*	73.15	18.5*	73.15	12.6*
	66.80	34.0*	92.2	27.5	85.85	14.0*
	79.50	35.8*	117.6	30.6	104.9	16.2
	130.30	43.1	143.0	33.8	143.5	20.7
	181.1	50.6	181.1	38.4	181.1	25.5
	231.9	57.8	257.3	47.4	231.9	31.6
SG Data	x	t[b]	x	t	x	t
	20.4	13.2,37.4	20.3	0.6	20.3	-[f]
	40.3	26.0,35.2	40.3	6.2	40.2	3.5
	59.2	32.5	59.3	7.3,13.3	59.3	-
	78.2	35.2	78.4	14.5,20.5	78.2	-
	97.4	36.7			97.4	15.2[f]
ℓ(mm)	41		104.9		47.8	
$^{29}\Delta t_D(\mu s)$	2		25.6		8.5	
$^{29}\Delta t_E(\mu s)$	12		42.6		9.5	
D(mm/μs)	7.0		8.3		8.3	
pre D(mm/μs)	0.54, 1.55		2.98		2.7	

---

* Custom-made probe.
a. All HMX is Class 1(A) from Batch X-906.
b. Increase in (dp/dt) or abrupt termination of record.
c. H95 Al
d. H-5 Al
e. F is failure to achieve steady state detonation.
f. Uncorrected baseline shift on these records.

Units of x are mm, of t, μs.

TABLE A1 (Cont'd)

DETAILED DATA FOR SHOTS

Shot No.	101C		103C		108C	
HE	80/20 HMX/Al[c]		70/30 HMX/Al[c]		60/40 HMX/Al[c]	
$\rho_o(\rho_v)$, g/cm^3	1.823(2.020)		1.859(2.086)		1.940(2.155)	
% TMD	90.2		89.1		90.0	

IP Data

x	t	x	t	x	t
22.35	0.0*	28.7	0.0*	28.7	0.0*
35.05	6.9*	47.75	12.7*	47.75	13.7*
47.75	11.2*	66.8	22.2*	60.45	18.0*
60.45	15.1*	85.85	27.9*	73.15	20.1*
73.15	15.7*	98.55	29.5*	85.85	21.5*
92.20	18.5	117.6	31.5	98.55	23.0*
117.6	21.8	143.0	34.5	111.25	24.35*
143.0	24.8	168.4	37.6	162.05	31.1
181.1	28.9	193.8	41.0	206.5	37.2
257.3	38.5	257.3	49.0	257.3	43.6

SG Data

x	t	x	t	x	t
20.3	1.8	20.5	4.3^f	40.3	Failed
40.3	5.7-8.6	40.1	6.4,13.4	59.2	to
56.8	12.6-16.2	59.2	16.8,23.7	78.5	Trigger
97.4	18.0-20.1	78.4	24.8-28.5	97.3	
		97.4	-	116.3	

	101C	103C	108C
ℓ(mm)	56.6	78.2	59.2
$^{29}\Delta t_D$(µs)	9.4	25.3	17.8
$^{29}\Delta t_E$(µs)	9.4	26.1	~17.8**
D(mm/µs)	8.3	8.0	7.7
pre D(mm/µs)	1.8,3.1	1.7,2.0	1.4, -

---

* Custom-made probe
** Estimated

c. H95 Al
f. Uncorrected baseline shift on these records.

TABLE A1 (Cont'd)

DETAILED DATA FOR SHOTS

Shot No.	111C		107C		112C	
HE	90/10 HMX/Al[d]		80/20 HMX/Al[d]		75/25 HMX/Al[d]	
$\rho_o(\rho_v)$, g/cm³	1.779(1.958)		1.828(2.020)		1.854(2.052)	
%TMD	90.9		90.5		90.4	
IP Data	x	t	x	t	x	t
	22.35	0.0*	28.7	0.0*	28.7	0.0*
	35.05	5.6*	41.4	8.1*	54.1	22.1*
	47.75	11.5*	54.1	13.8*	79.5	39.9*
	60.45	14.9*	66.8	19.8*	104.9	52.6*
	73.15	16.4*	79.5	26.0*	123.95	62.5*
	85.15	17.35*	92.2	31.1*	143.0	71.5
	104.9	19.75*	104.9	32.6*	162.05	75.3
	155.7	26.15	155.7	38.8	181.1	77.3
	206.5	32.35	206.5	45.6	219.2	82.1
	257.3	38.7	257.3	51.6	257.3	86.9
SG Data	x	t	x	t	x	t
	20.5	–	20.4	–[f]	20.7	10.0[f]
	40.1	2.7	40.3	3.0	66.7	24.2-30.8
	59.2	9.1-15.7	59.6	7.5-15.7	92.1	42.0
	78.5	11.9-20.0	78.2	15.7-26.5	117.7	48.7-57.7[f]
	97.3	–	97.3	27.4-33.2	143.0	65.2
ℓ(mm)	56.4		92.2		149.4	
$^{29}\Delta t_D$(µs)	10.8		31.0		74.0	
$^{29}\Delta t_E$(µs)	16.0		35.8		60.5	
D(mm/µs)	8.0		8.0		8.2	
pre D(mm/µs)	2.2		1.6,2.1		1.1-2.0,2.2	

---

* Custom-made probe

d. H-5 Al.

f. Uncorrected baseline shift on these records.

TABLE A1 (Cont'd)

DETAILED DATA FOR SHOTS

Shot No.	110C	106C
HE	70/30 HMX/A1[d]	60/40 HMX/A1[d]
$\rho_0(\rho_v)$, g/cm^3	1.885(2.086	1.956(2.155)
% TMD	90.4	90.8

IP Data

x	t
28.7	0.0*
47.75	16.4*
66.8	34.0*
85.85	50.7*
95.55	59.5*
117.60	68.2*
143.0	84.6
168.4	97.1
206.5	107.1
257.3	114.0

Instrumentation

Failed

SG Data

x	t
40.1	8
59.1	16.6,22.5
78.1	40.4
97.3	47-55.4[f]
116.5	Poor Record[f]

	110C	106C
ℓ(mm)	> 249(295**)	
$^{29}\Delta t_D$(µs)	> 114(120**)	
$^{29}\Delta t_E$(µs)	(120**)	
D(mm/µs)	F[e]	F
pre D(mm/µs)	1.1	

---

* Custom-made probe
** Estimated

d. H-5 A1.
e. F is failure to achieve steady state detonation.
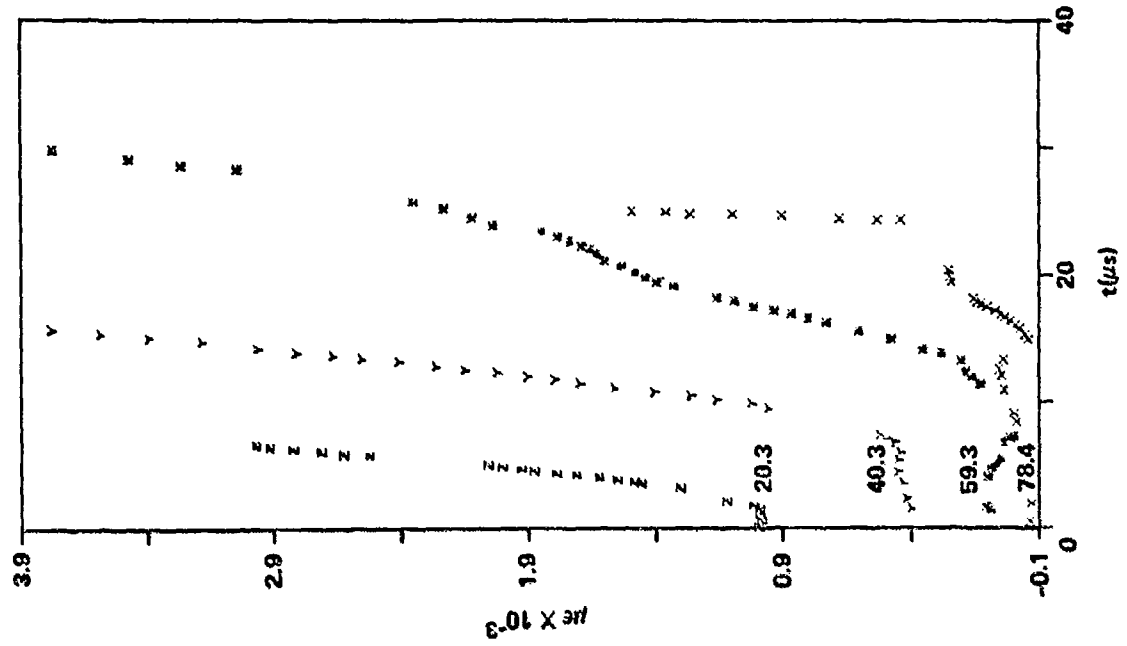f. Uncorrected baseline shift on these records.
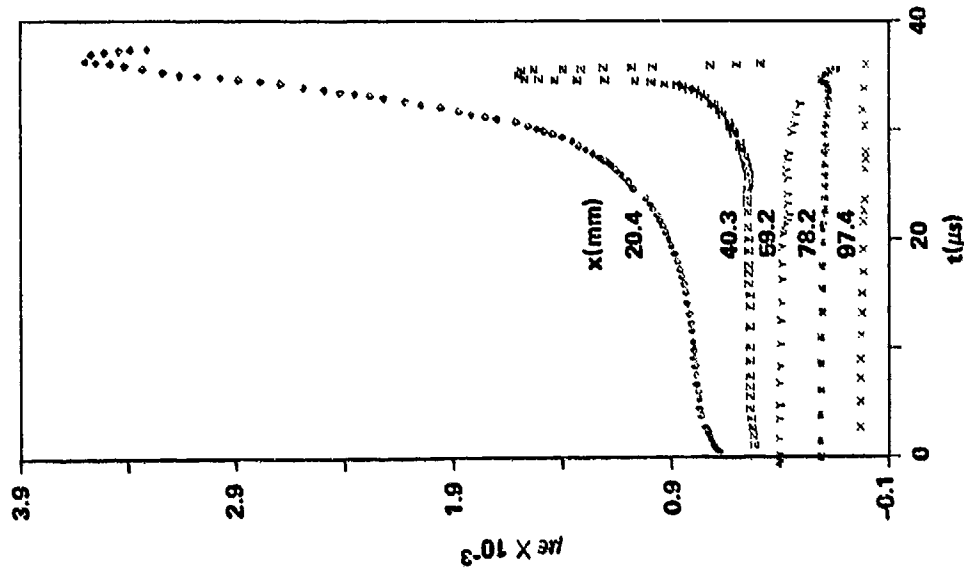
b. STRAIN-TIME DATA. (EACH CURVE, EXCEPT THE LOWEST, HAS BEEN RAISED 200μϵ – OR AN INTEGRAL MULTIPLE THEREOF – FOR BETTER DATA DISPLAY.)
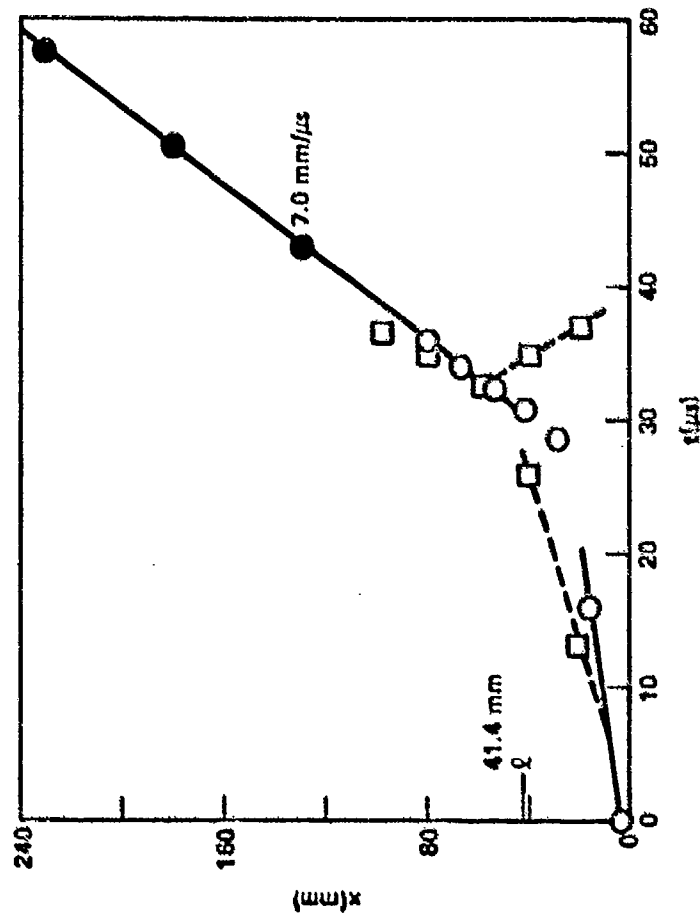
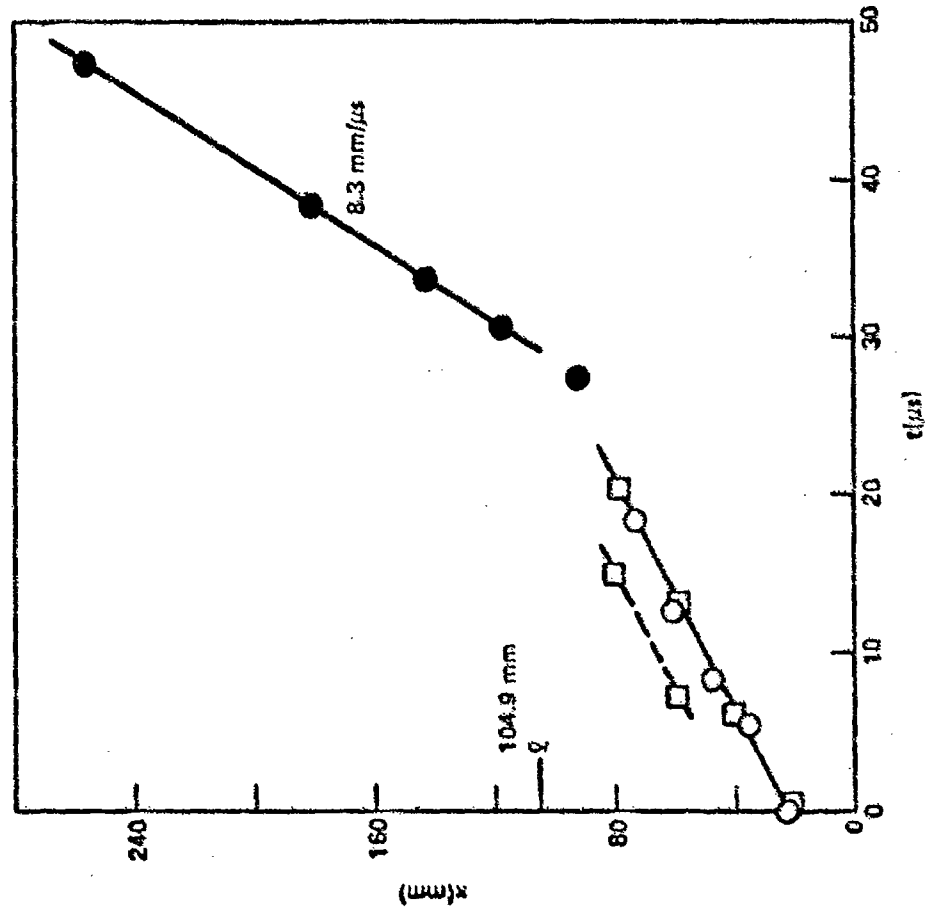a. DISTANCE-TIME DATA. (○ WOL PROBES, ● COMMERCIAL PROBES, □ SG EXCURSION TIME).

FIGURE A1   SHOT 109C ON 69.5% TMD HMX, ρ_o = 1.32 g/cm³.

b. STRAIN-TIME DATA.

a. DISTANCE-TIME DATA.

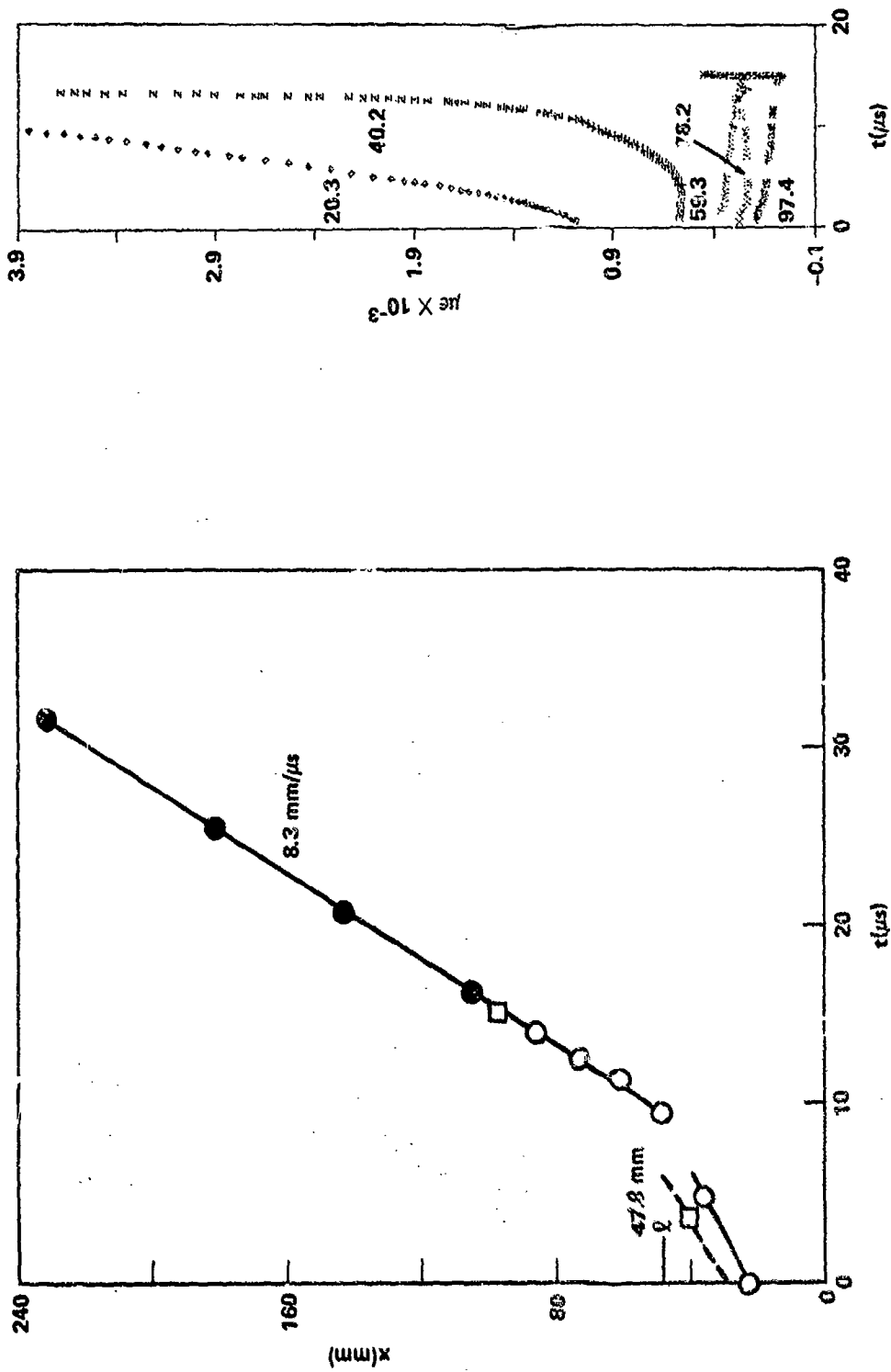FIGURE A2   SHOT 102C ON 89.5% TMD 90/10 HMX/95μ-AL, ρ_o = 1.76 g/cm³.   (KEYS OF FIGURE A1)

A-9

b. STRAIN-TIME DATA (UNCORRECTED BASELINE SHIFT IN RECORDS OF SGs AT 20.3 AND 97.4 mm).

a. DISTANCE-TIME DATA.

FIGURE A3   SHOT 113C ON 90.3% TMD 90/10 HMX/95μ-Al, ρ_0 = 1.77 g/cm^3.   (KEYS OF FIGURE A1)
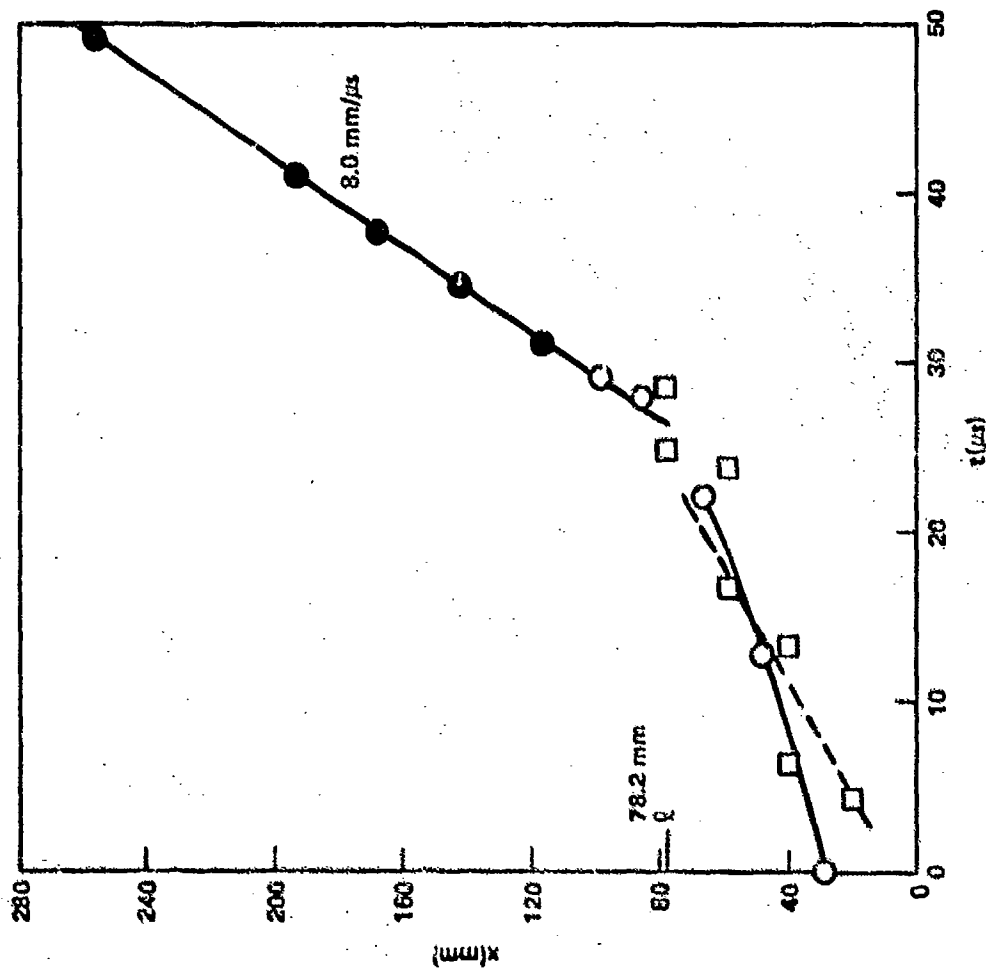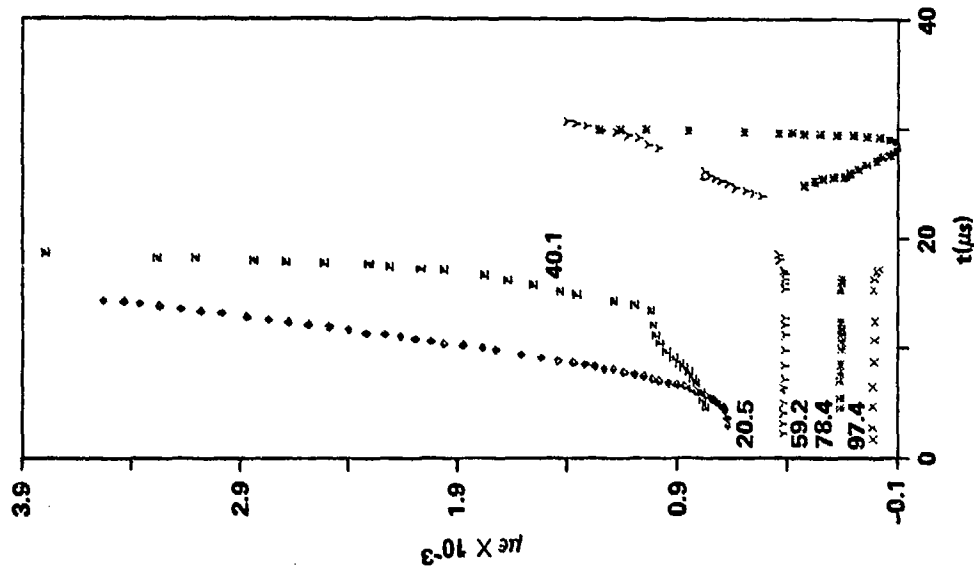
b. STRAIN-TIME DATA.

a. DISTANCE-TIME DATA.
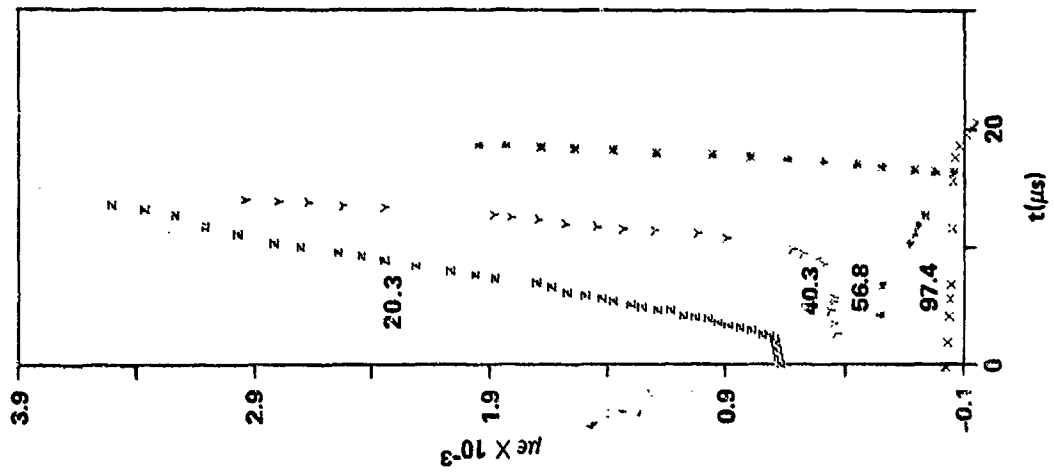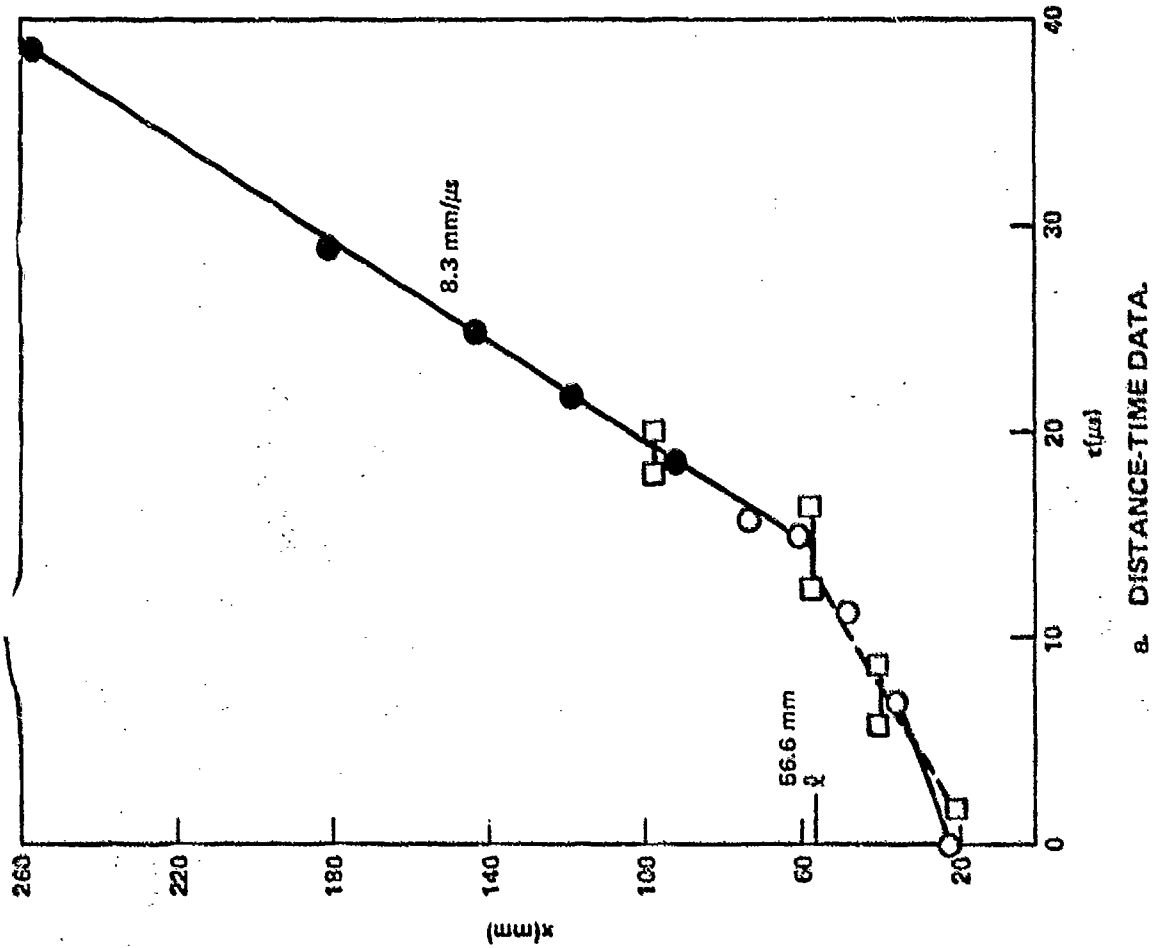
FIGURE A4   SHOT 101C ON 90.2% TMD 80/20 HMX/95μ-Al, ρ_o = 1.82 g/cm³. (KEYS OF FIGURE A1)

b. STRAIN-TIME DATA (UNCORRECTED BASELINE SHIFT IN RECORD OF SG AT 20.5 mm).

a. DISTANCE-TIME DATA.

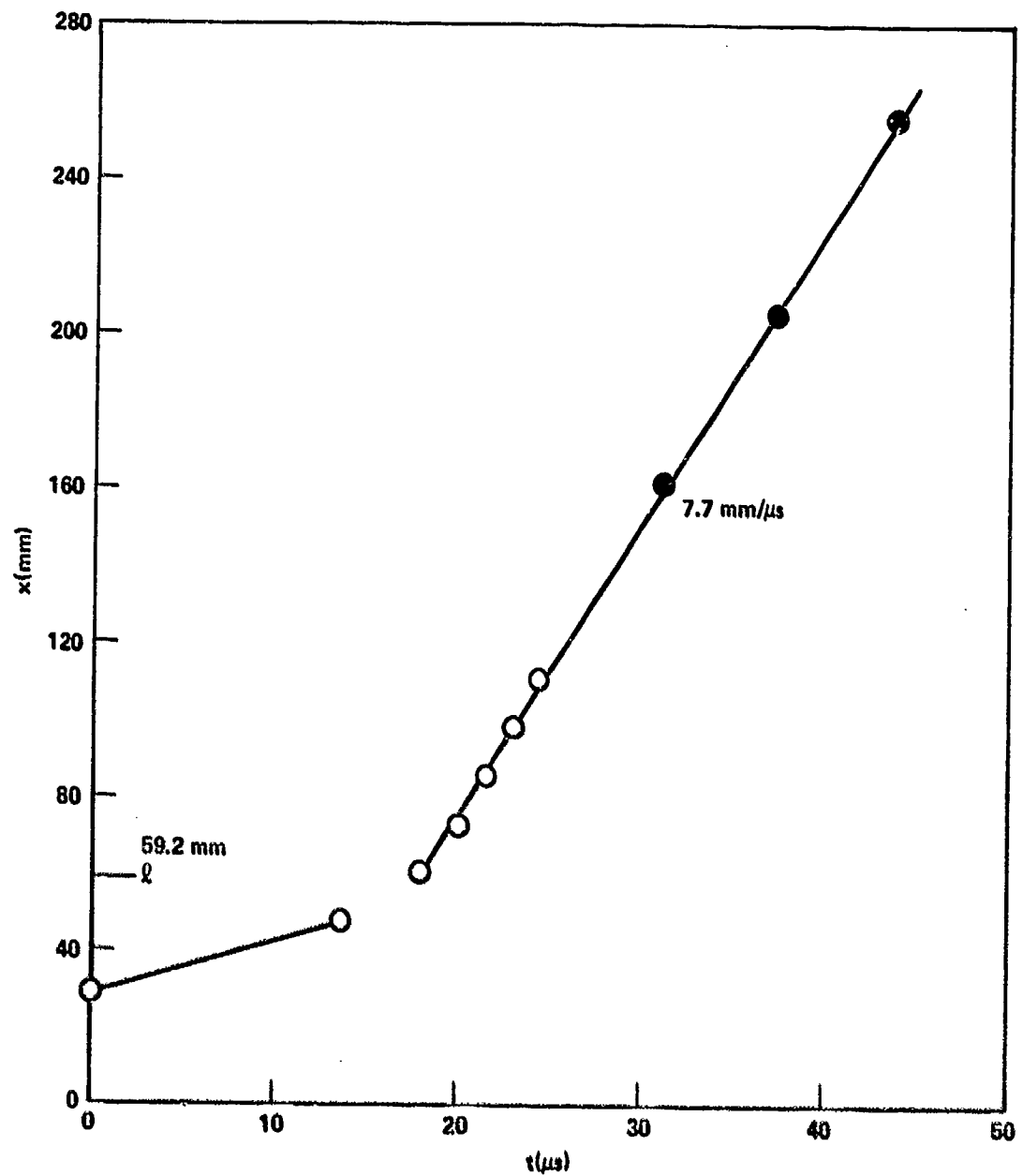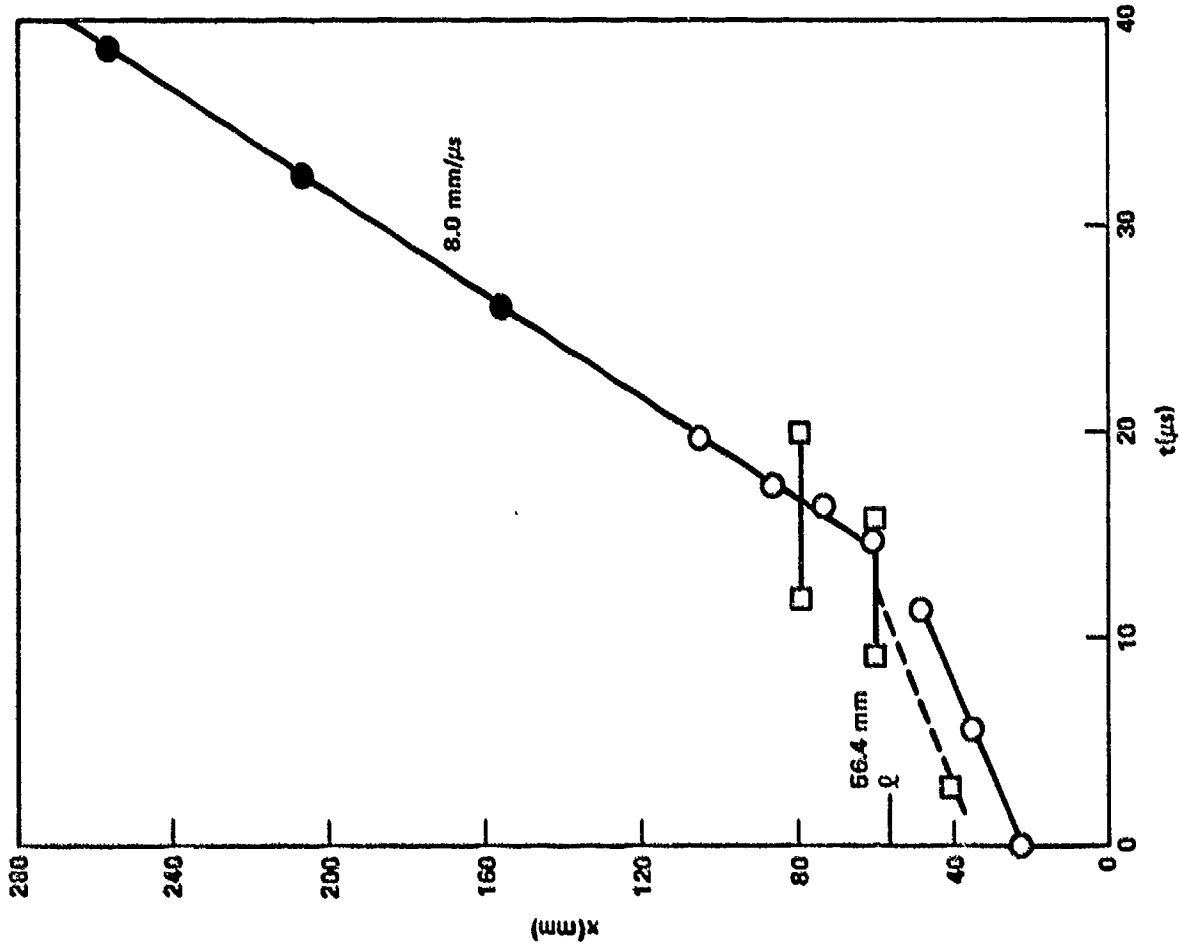FIGURE A5   SHOT 103C ON 89.0% TMD 70/30 HMX/95μ-Al, ρ_o = 1.86 g/cm^3. (KEYS OF FIGURE A1)
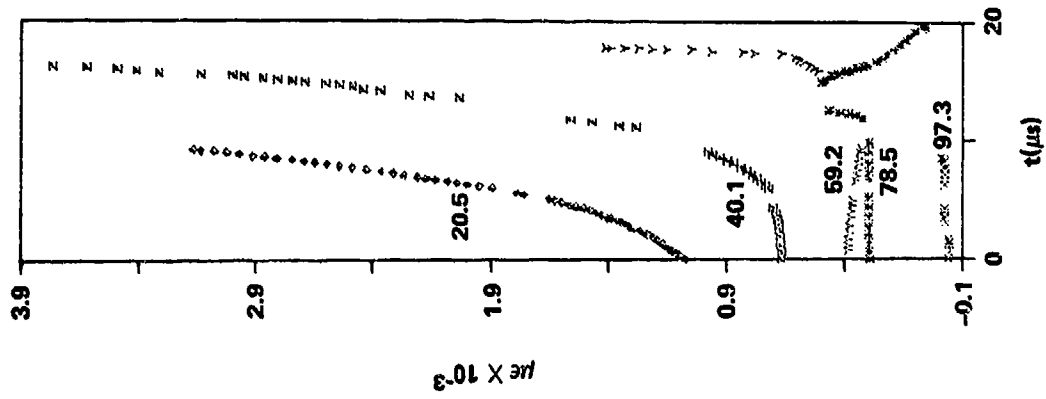
FIGURE A6   DISTANCE-TIME DATA FOR SHOT 108C ON 89.9%   TMD 60/40 HMX/95μ-Al,
ρ_0 = 1.94 g/cm^3. (KEYS OF FIGURE A1)

b. STRAIN-TIME DATA.

a. DISTANCE-TIME DATA.

FIGURE A7   SHOT 111C ON 88.9% TMD 90/10 HMX/5μ-Al, ρ_o = 1.78 g/cm³. (KEYS OF FIGURE A1)
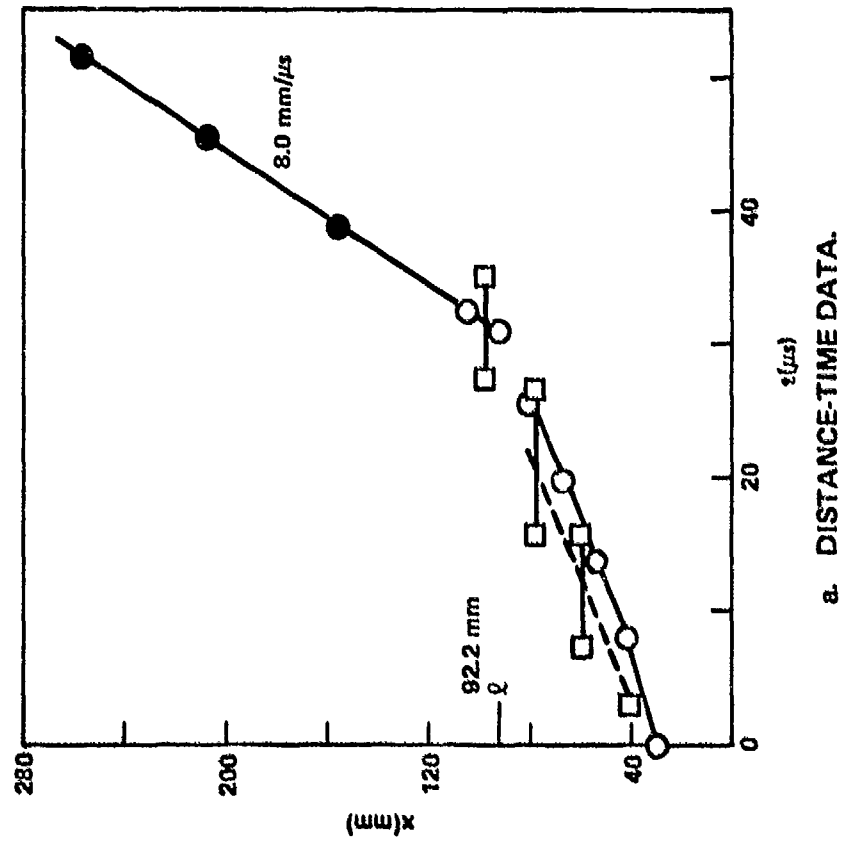
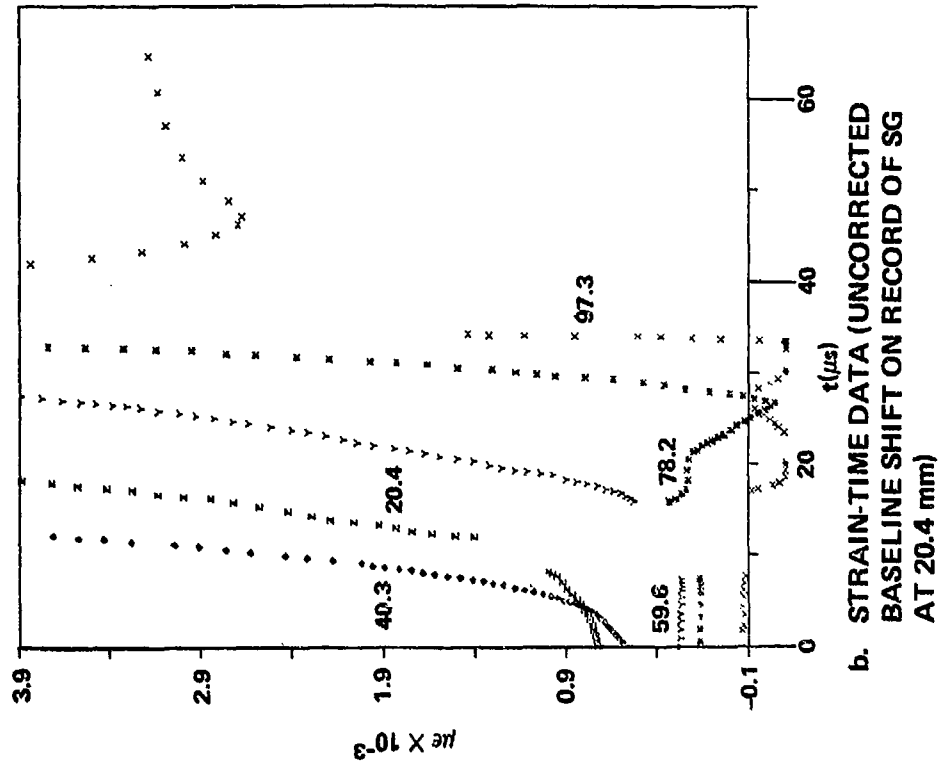b. STRAIN-TIME DATA (UNCORRECTED BASELINE SHIFT ON RECORD OF SG AT 20.4 mm)

a. DISTANCE-TIME DATA.

FIGURE A8   SHOT 107C ON 90.4% TMD 80/20 HMX/5μ-Al, ρ_o = 1.83 g/cm^3. (KEYS OF FIGURE A1)

A-15

b. STRAIN-TIME DATA (UNCORRECTED BASELINE SHIFT ON RECORDS OF SGs AT 10.7 AND 117.7 mm).

a. DISTANCE-TIME DATA.
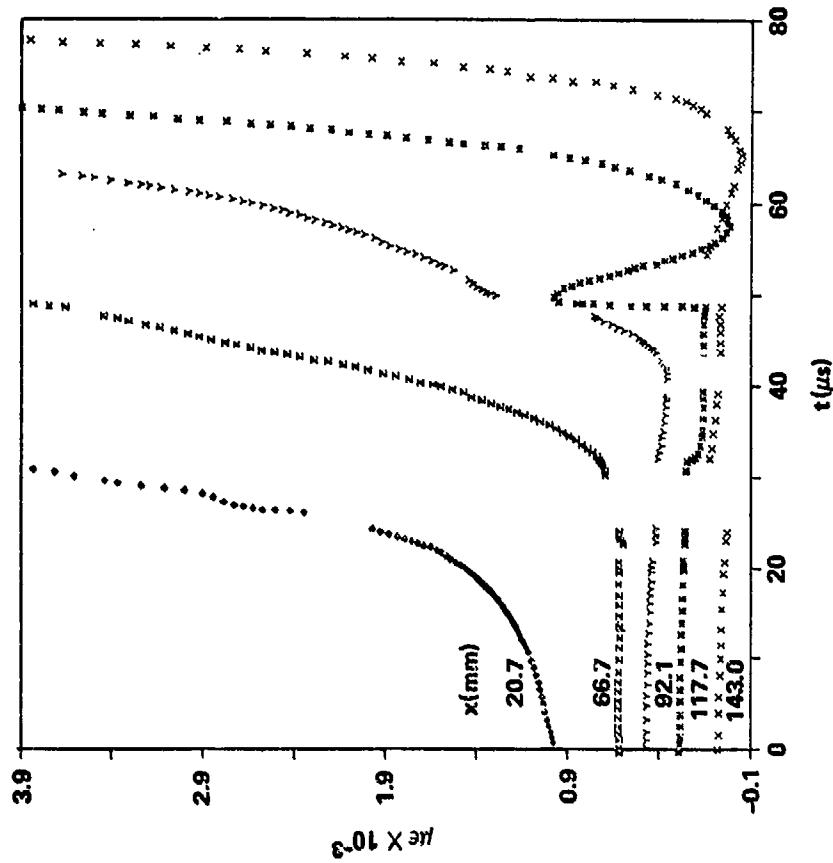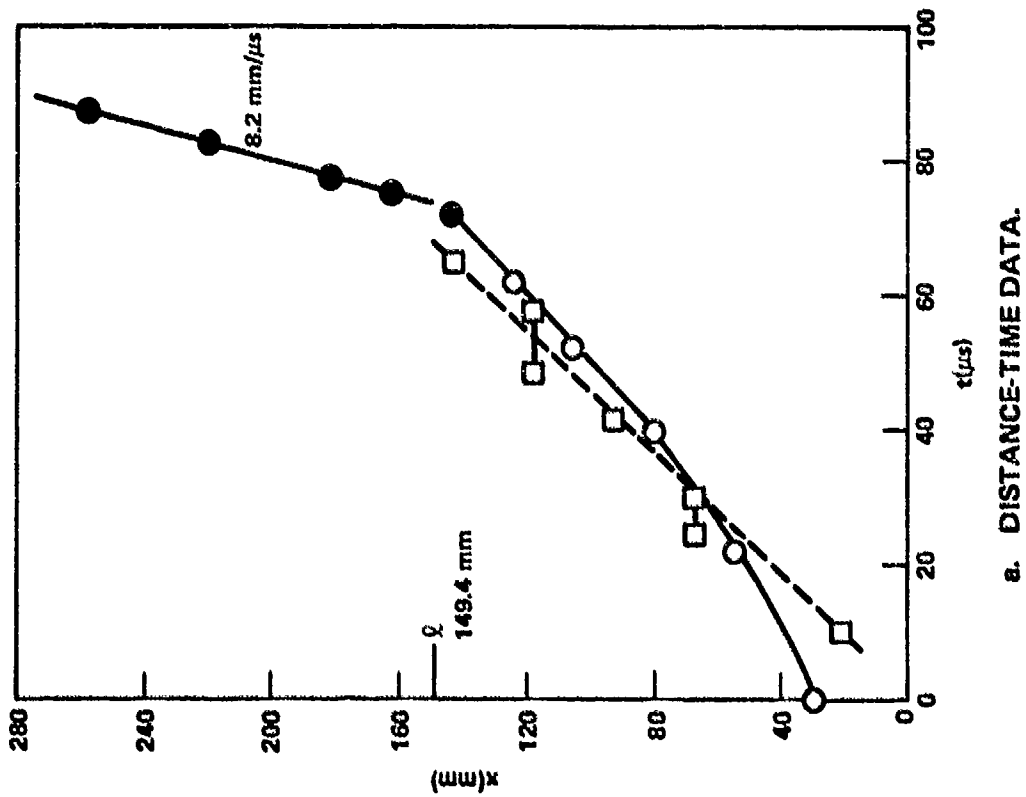
FIGURE A9   SHOT 112C ON 90.3% TMD 75/25 HMX/5μ-AI, ρ_o = 1.85 g/cm³.   (KEYS OF FIGURE A1)
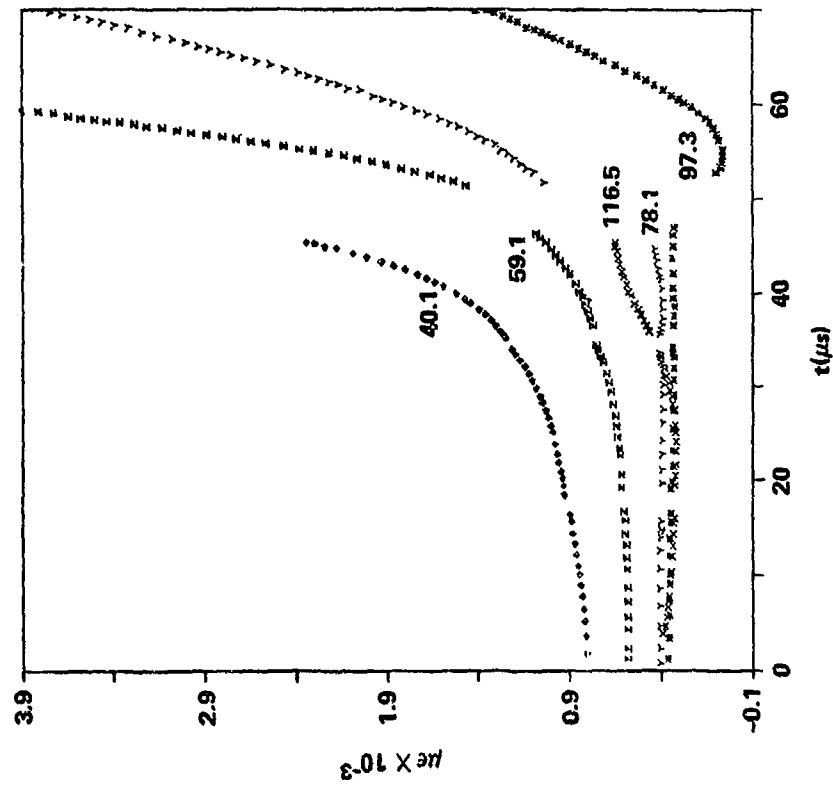
b. STRAIN-TIME DATA (UNCORRECTED BASELINE SHIFT ON RECORDS OF SGs AT 97.3 AND 116.5 mm).
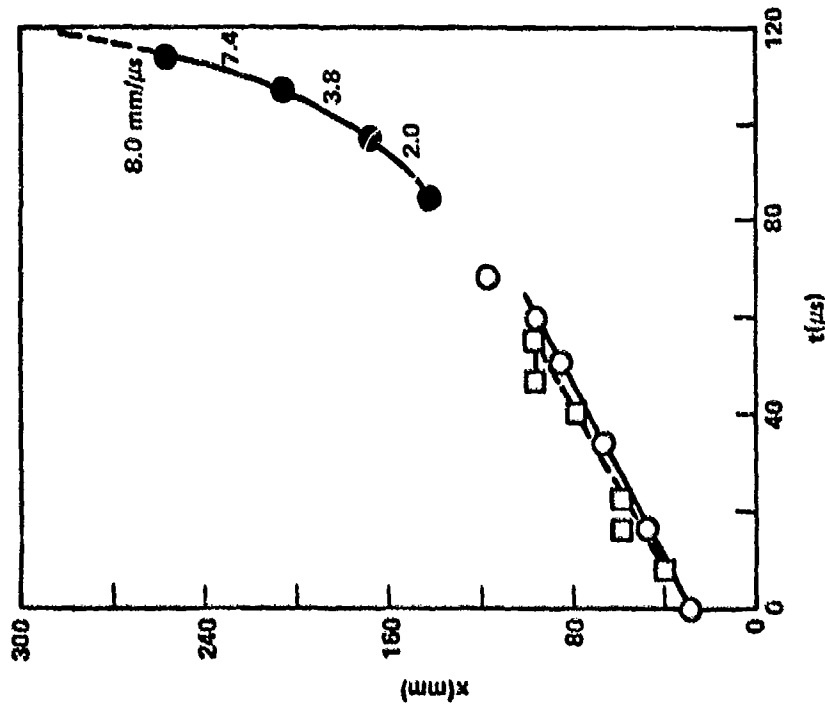
a. DISTANCE-TIME DATA.

FIGURE A10 SHOT 110C ON 90.3% TMD 70/30 HMX/5μ-Al, ρ_o = 1.89 g/cm³. (KEYS OF FIGURE A1)

c. 70/30 HMX/Al
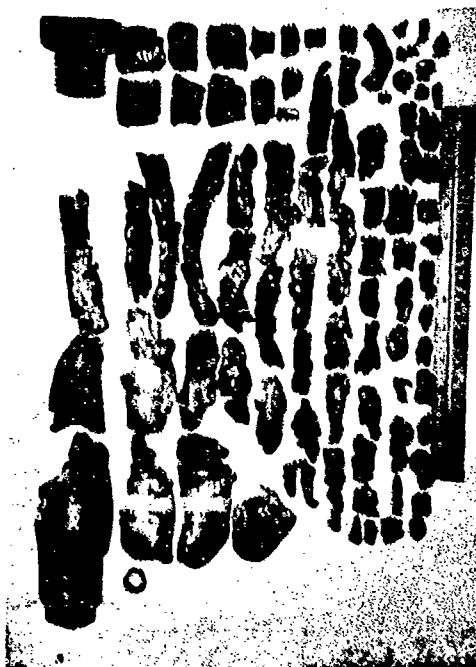
d. 60/40 HMX/Al

a. 90/10 HMX/Al

b. 75/25 HMX/Al

FIGURE A11 REPRESENTATIVE PHOTOGRAPHS OF FRAGMENT DISTRIBUTION FROM THE ALUMINIZED (5μAl) HMX.

DISTRIBUTION

Chief of Naval Material
Washington, DC   20360

Commander
Naval Air Systems Command
Attn: AIR-350
        AIR-330
Department of the Navy
Washington, DC   20361

Commander
Naval Sea Systems Command
Attn: Technical Library
        SEA-03B
        SEA-62R
        SEA-62R2
        SEA-62R3
        SEA-62R32
        SEA-64E
Department of the Navy
Washington, DC   20362

Director
Strategic Systems Project Office (PM-1)
Attn: SP-273 (R. M. Kinert)
        SP-27311 (E. L. Throckmorton, Jr.)
Department of the Navy
Washington, DC   20376

Office of Naval Research
Attn: Rear Admiral C. O. Holmquist
        ONR-741 (Technical Library)
Department of the Navy
Arlington, VA   22217

2

DISTRIBUTION (Cont.)

Commander
Naval Weapons Center
Attn: Code 556
        Technical Library
        H. D. Mallory
        Code 452
        Code 5008
        R. L. Derr   2
China Lake, CA 93555

Director
Naval Research Laboratory
Attn: Technical Information Section   2
Washington, DC 20375

Office of Chief of Naval Operations
Operations Evaluation Group (OP03EG)
Washington, DC 20350

Director
Office of the Secretary of Defense
Advanced Research Projects Agency
Washington, DC 20301

Scientific and Technical
  Information Facility, NASA
P. O. Box 33
College Park, MD 20740

Commanding Officer
Naval Weapons Station
Attn: R&D Division
        Code 50
Yorktown, VA 23691

Commanding Officer
Naval Propellant Plant
Attn: Technical Library
Indian Head, MD 20640

Commanding Officer
Naval Explosive Ordnance Disposal Facility
Attn: Information Services
Indian Head, MD 20640

McDonnell Aircraft Company
Attn: M. L. Schimmel
P. O. Box 516
St. Louis, MO 63166

DISTRIBUTION (Cont.)

Commanding Officer
Naval Ammunition Depot
Crane, IN 47522

Commanding Officer
Naval Underwater Systems Center
Attn: LA 151-Technical Library
Newport, RI 02840

Commanding Officer
Naval Weapons Evaluation Facility
Attn: Code AT-7
Kirtland Air Force Base
Albuquerque, NM 87117

Commanding Officer
Naval Ammunition Depot
Attn: QEL
Concord, CA 94522

Superintendent Naval Academy
Attn: Library
Annapolis, MD 21402

Naval Plant Representative Office
Strategic Systems Project Office
Lockheed Missiles and Space Company
Attn: SPL-332 (R. H. Guay)
P. O. Box 504
Sunnyvale, CA 94088

Hercules Incorporated
Allegany Ballistics Laboratory
Attn: Library
P. O. Box 210
Cumberland, MD 21502

AMCRD
5001 Eisenhower Avenue
Alexandria, VA 22302

Redstone Scientific Information Center
U. S. Army Missile Command
Attn: Chief, Documents
Redstone Arsenal, AL 35809

2

DISTRIBUTION (Cont.)

Commanding Officer
Army Armament Research and
  Development Command
Energetic Materials Division
Attn: Louis Aurami, DRDAR-LCE
Dover, NJ 07801

Commanding General
Attn: BRL
Aberdeen Proving Ground, MD 21005

Commanding Officer
Harry Diamond Laboratories
Attn: Library
2800 Powder Mill Road
Adelphi, MD 20783

Armament Development & Test Center
DLOSL/Technical Library
Eglin Air Force Base, Florida 32542

Commanding Officer
Naval Ordnance Station
Louisville, KY 40124

Director
Applied Physics Laboratory
Attn: Library
Johns Hopkins Road
Laurel, MD 20810

U. S. Department of Energy
Attn: DMA
Washington, DC 20545

Director
Defense Nuclear Agency
Washington, DC 20305   2

Research Director
Pittsburgh Mining and Safety
  Research Center
Bureau of Mines
Attn: R. W. Van Dolah
4800 Forbes Avenue
Pittsburgh, PA 15213

DISTRIBUTION (Cont.)

Director
Defense Documentation Center
Cameron Station
Alexandria, VA 22314   12

Goddard Space Flight Center, NASA
Glenn Dale Road
Greenbelt, MD 20771

Lawrence Livermore Laboratory
University of California
Attn: M. Finger
       E. James
       E. Lee
       P. Urtiew
P. O. Box 808
Livermore, CA 94551

Sandia Laboratories
Attn: R. J. Lawrence, Div. 5166
P. O. Box 5800
Albuquerque, NM 87115

Director
Los Alamos Scientific Laboratory
Attn: Library
       L. C. Smith
       B. G. Craig
       A. Popolato
P. O. Box 1663
Los Alamos, NM 87544

DDESB
Forrestal Building, Room GS 270
Washington, DC 20314

Aerojet Ordnance and Manufacturing
  Company
9236 East Hall Road
Downey, CA 90241

Hercules Incorporated Research Center
Attn: Technical Information Division
       B. E. Clouser
Wilmington, DE 19899

DISTRIBUTION (Cont.)

Thiokol/Huntsville Division
Attn: Technical Library
Huntsville, AL 35807

Shock Hydrodynamics Division
Whittaker Corporation
Attn: Dr. L. Zernow
4716 Vineland Avenue
North Hollywood, CA 91602

Stanford Research Institute
Attn: D. Curran
       C. M. Tarver
333 Ravenswood Avenue
Menlo Park, CA 94025

Thiokol/Wasatch Division
Attn: Technical Library
P. O. Box 524
Brigham City, UT 84302

Thiokol/Elkton Division
Attn: Technical Library
P. O. Box 241
Elkton, MD 21921

Teledyne McCormick Selph
P. O. Box 6
Hollister, CA 95023

Lockheed Missiles and Space Division
1122 Jagels Road
Sunnyvale, CA 94086

R. Stresau Laboratory, Inc.
Star Route
Spooner, WI 54801

Rohm and Haas
Huntsville, Defense Contract Office
Attn: H. M. Shuey
723-A Arcadia Circle
Huntsville, AL 35801

2

6

DISTRIBUTION (Cont.)

U. S. Army Foreign Service
  and Technology Center
220 7th Street, N.E.
Charlottesville, VA   22901

Princeton University
Department of Aerospace and
  Mechanical Sciences
Attn: M. Summerfield
Princeton, NJ   08540

Pennsylvania State University
Department of Mechanical Engineering
Attn: K. Kuo
University Park, PA   16802

Ballistic Research Laboratories
Attn: N. Gerri
Aberdeen Proving Ground, MD   21005

Paul Gough Associates
1048 South Street
Portsmouth, NH   03801

Hercules Incorporated, Bacchus Works
Attn: B. Hopkins
P. O. Box 98
Magna, UT   84044

Professor H. Krier
A & A Engineering Department
101 Transportation Building
University of Illinois
Urbana, IL   61801

Chemical Propulsion Information Agency
The Johns Hopkins University
Applied Physics Laboratory
Johns Hopkins Road
Laurel, MD   20810

IIT Research Institute
Attn: H. S. Napadensky
10 West 35th Street
Chicago, IL   60616

DISTRIBUTION (Cont.)

Erion Associates, Inc.
Attn: W. Petray
600 New Hampshire Avenue,
  Suite 870
Washington, DC 20037

Brigham Young University
Department of Chemical Engineering
Attn: Dr. M. W. Beckstead
Provo, UT 84601

TO AID IN UPDATING THE DISTRIBUTION LIST
FOR NAVAL SURFACE WEAPONS CENTER, WHITE
OAK TECHNICAL REPORTS PLEASE COMPLETE THE
FORM BELOW:

TO ALL HOLDERS OF ___NSWC/TR 79-119___
by Donna Price, Code R-13
DO NOT RETURN THIS FORM IF ALL INFORMATION IS CURRENT

A. FACILITY NAME AND ADDRESS (OLD) (Show Zip Code)

NEW ADDRESS (Show Zip Code)

B. ATTENTION LINE ADDRESSES:

C.

☐ REMOVE THIS FACILITY FROM THE DISTRIBUTION LIST FOR TECHNICAL REPORTS ON THIS SUBJECT.

D.
NUMBER OF COPIES DESIRED _____

DEPARTMENT OF THE NAVY
NAVAL SURFACE WEAPONS CENTER
WHITE OAK, SILVER SPRING, MD. 20910

OFFICIAL BUSINESS
PENALTY FOR PRIVATE USE, $300

POSTAGE AND FEES PAID
DEPARTMENT OF THE NAVY
DOD 316

COMMANDER
NAVAL SURFACE WEAPONS CENTER
WHITE OAK, SILVER SPRING, MARYLAND 20910

ATTENTION: CODE R-13